

A Detailed Model to Determine the Effective Solar Optical Properties of Draperies

Nathan A. Kotey
Student Member ASHRAE

John L. Wright, PhD, PEng
Member ASHRAE

Michael R. Collins, PhD
Associate Member ASHRAE

ABSTRACT

Drapes have the potential to reduce peak cooling load and annual energy consumption because they can be used to control solar gain. Thus, the need to model a drapes in a glazing system analysis is important. A detailed model that can be used to estimate the spatially averaged (effective) solar optical properties of a drapery is presented. This model approximates a drapery as a series of uniformly arranged rectangular pleats. The effective solar optical properties of the drapery are then determined by considering a representative enclosure. The solar properties of the fabric are incidence angle dependent, and the effects of beam and diffuse components, in both reflection and transmission, are included. Furthermore, the model can be applied to fabrics with differing front and back properties. The model therefore offers new possibilities in calculating the effective solar optical properties of draperies made with practically any fabric. Results are presented for both incident beam and diffuse radiation.

INTRODUCTION

Draperies provide privacy, reduce glare, and improve aesthetics. Draperies can also be used to reduce solar gain, peak cooling load, and annual energy consumption. The energy performance for windows with shading devices can be modeled using a two-step procedure. In the first step, solar radiation is considered. This requires the determination of the solar optical properties of each layer in the glazing/shading system. Layers that are not uniform (e.g., shading layers) are assigned spatially averaged, or “effective,” solar optical properties. Assigning effective optical properties to a shading layer allows it to be treated as a homogeneous, planar layer that can be placed at any location with respect to the glazing system.

The effective properties can then be used as part of a multilayer analysis that considers beam and diffuse components of solar radiation as they interact with a multilayer assembly (e.g., Wright and Kotey [2006]). This procedure provides calculated values of system solar transmission and absorbed solar components. The absorbed solar components appear as energy source terms in the second step—the heat transfer analysis (e.g., Wright [2008]).

Researchers have used several ways to quantify the reduction of solar gain when draperies are present. Keyes (1967), for example, characterised fabrics by yarn colour (yarn reflectance) as dark (D), medium (M), and light (L) and by weave as open (I), semi-open (II), and closed (III). Keyes then developed a chart that expressed measured shading coefficient (SC), defined as the ratio of solar gain through a window to the solar gain through a standard layer of clear glass as a function of yarn reflectance and weave openness when a drapery was combined with both regular plate and heat-absorbing glass. If the solar optical properties of the fabric are not well known, the Keyes method can still be used to obtain an approximate SC of the glass-drapery combination.

Having acknowledged that fabric colour and weave openness alone were not sufficient to accurately determine the SC of the glass-drapery combination, Moore and Pennington (1967) developed a chart that expressed the SC as a function of fabric solar optical properties. They measured the solar optical properties of fabrics, draperies, and glass-drapery combinations using various techniques. They also measured the SC using a solar calorimeter. Furthermore, they developed equations to calculate the SC using solar optical properties as inputs. The effective solar properties of the drapery were estimated by applying a multiplicative factor to the solar proper-

Nathan A. Kotey is a graduate student, **John L. Wright** is a professor, and **Michael R. Collins** is an associate professor in the Department of Mechanical and Mechatronics Engineering, University of Waterloo, Waterloo, Ontario, Canada.

ties of the fabric at normal incidence. This factor accounted for the effect of folding and the variation of incidence angle. Their calculations agreed well with experimentally determined SC values.

By careful analysis of fabric transmittance and reflectance, yarn reflectance, and openness factor, Keyes (1967) was able to reconcile the yarn reflectance-openness chart with the fabric reflectance-transmittance chart. The Keyes (1967) universal chart is the basis of the interior attenuation coefficient (IAC) data for glass-drapery combinations found in the 2005 *ASHRAE Handbook—Fundamentals* (ASHRAE 2005). This chart correlates measured optical properties with eye-observed values to determine the IAC, thus making it a convenient tool for designers. However, optical properties measurements carried out by Moore and Pennington (1967) revealed that the solar properties could differ from the visible properties. In such situations, using visual judgement to predict shading effects could give inaccurate results.

The first attempt to quantify the cumulative effect of folding (or pleating) and the directional nature of incident radiation on the solar gain through draperies was carried out by Ozisik and Schutrum (1960). To determine the effectiveness of 100% fullness draperies in reducing solar gain, Ozisik and Schutrum tested draperies of different fabrics in combination with regular and heat-absorbing glass using a solar calorimeter. Their results were presented in terms of the solar heat transfer factor K , defined as the ratio of the solar gain to insolation. Note that K is identical to the solar heat gain coefficient (SHGC) currently used. They showed that K was independent of incidence angle for incidence angles ranging from 0° to 50° . For incidence angles greater than 50° , they suggested a decrease in K by 10% for each 10° increase in incidence angle. They also proposed a reduction of 10% in K for incident diffuse radiation. Furthermore, they presented the variation of K with solar optical properties of fabrics at normal incidence and observed that the reflectance was the dominant property influencing solar gain. In addition to the solar gain tests, they performed a series of tests to investigate the effect of pleating on the solar optical properties of draperies. They measured the angular transmittance and reflectance of both fabrics and draperies with a pyrhelimeter. Their results showed that the transmittance of the drapery at normal incidence was almost the same as that of the fabric. However, at 45° incidence, the transmittance of the drapery was 20% lower. For incident diffuse radiation, both transmittance and reflectance of the drapery were 20% lower than the fabric values.

Yellot (1965) determined experimentally the solar heat gain factor (SHGF), defined as solar gain through a standard clear glass, and the SC of draperies using an outdoor solar calorimeter. He also measured the solar optical properties of fabrics as well as glass-fabric combinations using a custom-made instrument. The measurements were taken at incidence angles ranging from 26° to 90° . His experiments showed that the SHGC for a typical glass-fabric combination decreased as the incidence angle increased, although the SC remained

nearly constant. To explore the effects of varying surface solar azimuth on reflectance, Yellot used a reflectometer to measure the reflectance of a typical light-coloured fabric and drapery. His results showed that although the reflectance of both fabric and drapery varied with surface solar azimuth, there was very little difference between the two reflectances for a given surface solar azimuth.

The results of the preceding studies (Keyes 1967; Moore and Pennington 1967; Ozisik and Schutrum 1960; Yellot 1965) are useful in predicting the solar gain through windows with draperies. However, they are limited to single-glazed windows.

Few data can be found in the literature for comparison against results of the research presented in this study. The work of Farber et al. (1963) is of particular interest because it includes a model to determine the effective solar optical properties of draperies using a simplified rectangular configuration. Farber et al. assumed that the fabric is diffusely reflecting and diffusely transmitting and that the reflectance and transmittance for beam radiation vary with incidence angle. Their calculation involved separate treatments of the front and the cavity portions of the pleated drapery, with the front portion having the same optical properties as the fabric. The solutions of the cavity portion and the front portion were averaged to give the effective optical property of the drapery. Farber et al. used results published by Sparrow and Johnson (1962) to estimate the apparent (i.e., effective) reflectivity of the cavity portion of the drapery, noting that these results were obtained by means of “long and tedious numerical computer techniques.” It was also asserted, without explanation, that the abnormal transmittance of the pleated drapery follows the same pattern as the abnormal reflectance. In addition, examining the work of Sparrow and Johnson, it can be seen that the reflectance of the cavity portion of the drapery (with respect to beam insolation) was estimated on the assumption that each groove is infinitely deep. However, by examining Figure 7 of Sparrow and Johnson’s study, it is apparent that this assumption is not valid. Pennington et al. (1964), while using the model of Farber et al. to compare against measurements, mention that:

If a zero deg horizontal projection angle had been assumed for the rectangular configuration of the theoretical analysis, then the curves of absorptance, reflectance and transmittance versus incidence angle would have been identical to that of a flat drapery.

This statement offers additional insight regarding the limitations of the Farber et al. model. The Farber et al. model is unable to account for the effect of pleating when solar radiation is incident normal, or near normal, to the window.

To validate the theoretical analysis carried out by Farber et al. (1963), Pennington et al. (1964) performed a series of experiments with an outdoor solar calorimeter. They used a pyrhelimeter installed in the calorimeter to measure the solar optical properties of fabrics, draperies, and glass-drapery

combinations at various incidence (or profile) angles. Regarding the results for pleated draperies, Pennington et al. note:

In general, the two methods show good agreement on transmittance. Their agreement, however, on reflectance and absorptance leaves much to be desired.

These discrepancies are not surprising given the range of assumptions used by Farber et al. and the method used to account for the interaction of solar radiation with the groove portion of the drapery. These researchers were clearly hampered by limitations in theory and computational power available at the time. Nonetheless, calculated results from Farber et al. (1963) are subsequently presented and compared with the model developed in the current study.

A recent study by Kotey et al. (2007) modeled a drapery layer as a series of rectangular pleats with diffusely transmitting and diffusely reflecting fabric. This model assumed that the fabric solar optical properties were independent of the angle of incidence and did not allow for direct beam transmission of solar radiation through openings in the drapery fabric. The effective solar optical properties of the drapery were then determined as a function of drapery geometry and solar profile angle. This simplified approach has been extended in this study to include several additional effects. In particular, the pleated drape model presented here makes use of fabric properties that are determined as a function of incidence angle—these properties including detail regarding beam and diffuse components of reflection and transmission. It is assumed that these properties are available with respect to both beam and diffuse insolation. The methods for determining all of these fabric properties have been developed in a concurrent study, and the fabric property models used in this study of pleated drapes are documented in a companion publication (Kotey et al. 2009).

OBJECTIVE

The main objective of this research is to develop a detailed effective solar optical properties model for pleated draperies with the aim of using this model in building energy simulation. Previous research considered diffusely transmitting and diffusely reflecting fabrics with properties that were independent of incidence angle. Such restrictions have been removed by considering both beam-beam and beam-diffuse transmission of both the fabric and the pleated drapery. Furthermore, semi-empirical models expressing the variation of fabric properties with incidence angle have been incorporated (Kotey et al. 2009).

MODELING

The effective solar optical properties of a drapery are dependent on many things, including the colour of the yarn, the openness of the fabric, the pleat geometry, and the direction of the incident solar radiation. The model presented in this study was developed in an attempt to account for all of these influences. Pleat geometry is approximated as rectangular and

self shading and, along with the directional characteristics of the fabric, has an important influence on the effective properties of the pleated drape. The solar properties of a fabric are dependent on the openness of the weave as well as the colour of the yarn and the directional nature of the incoming radiation. For a given fabric, experiments show that the solar optical properties pertaining to beam radiation at off-normal incidence can be determined using properties measured at normal incidence. Solar optical properties pertaining to incident diffuse radiation can also be determined. Details of the experimental procedure and the resulting fabric property models are given in Kotey et al. (2009).

Drape Geometry and Solar Angles

A drape consists of a series of fabric pleats that are non-uniform. Similar to the approach used by Farber et al. (1963), rectangular pleats were used in this study as an approximation (see Figure 1). Consider beam radiation incident on the drapery. The interception of the beam radiation by fabric surfaces is dependent on the angle of incidence, θ . In addition, the perpendicular surfaces of the drapery can produce considerable blockage. The blockage is influenced by pleat geometry and horizontal profile angle, Ω_H (equivalent to the surface solar azimuth). If the fabric properties are influenced by (local) incidence angle, the vertical profile angle, Ω_V , also comes into play. The relationship between θ , Ω_H , and Ω_V is well documented (e.g., ASHRAE [2005]). For fabric surfaces parallel and perpendicular to the window, it can be shown that

$$\cos(\theta_{PARL}) = \cos[\tan^{-1}(\tan\Omega_V \cos\Omega_H)] \cdot \cos\Omega_H \quad (1)$$

and

$$\cos(\theta_{PERP}) = \cos[\tan^{-1}(\tan\Omega_V \sin\Omega_H)] \cdot \sin\Omega_H, \quad (2)$$

where θ_{PARL} and θ_{PERP} are the incidence angles on the parallel and perpendicular surfaces, respectively.

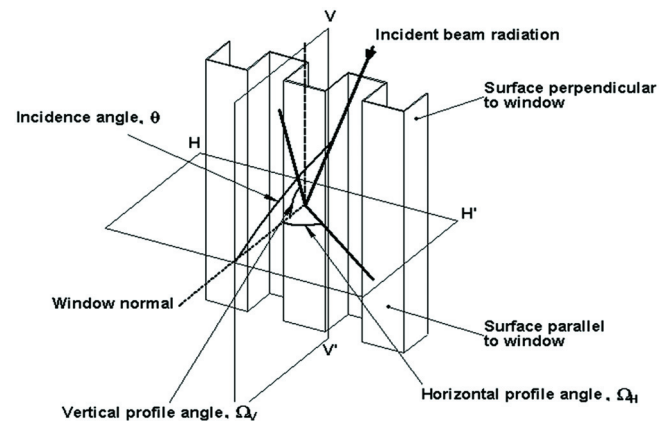


Figure 1 Configuration of drapery model showing solar angles.

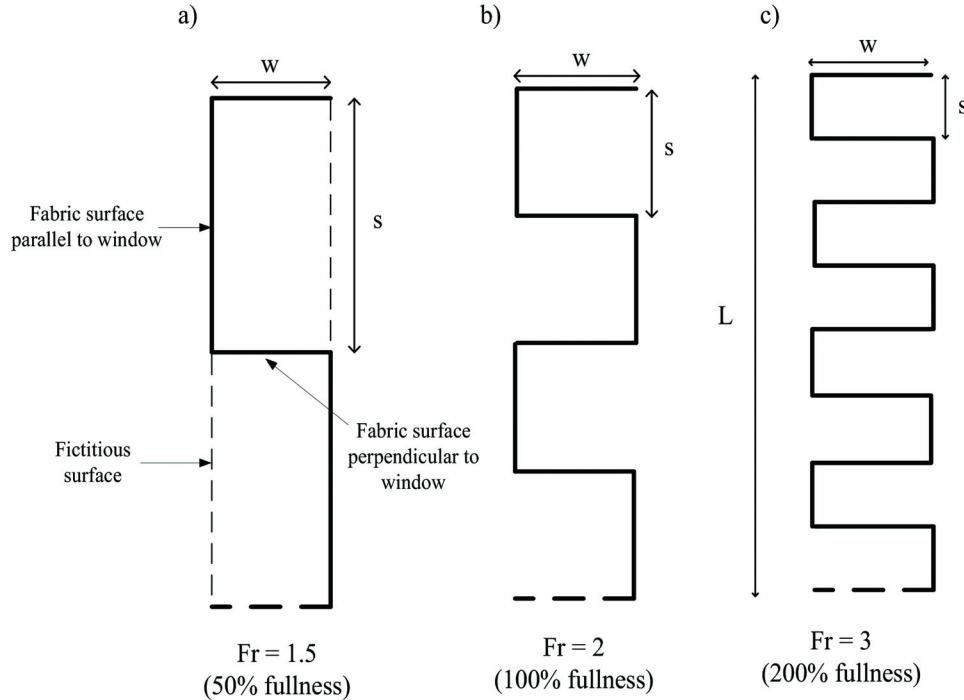


Figure 2 Cross-section of drapery pleats with different values of folding ratio and percent fullness.

Since the pleats are repetitive, an enclosure formed by two consecutive pleats will represent the entire drapery. A cross-section of such an enclosure is shown in Figure 2a. The representative enclosure is made up of two sub-enclosures with pleat width w and pleat spacing s . Fictitious surfaces at the front and back openings complete the enclosure.

The solar optical properties of the drapery are influenced by pleat geometry, which can be described in terms of folding ratio, Fr , or percent fullness. The folding ratio is defined as the total length of the fabric divided by the length of the drapery, L . When the length of the fabric is twice that of the drapery, $Fr = 2$, the drapery is described as having 100% fullness. Figures 2a, 2b, and 2c show draperies with different values of Fr and fullness. The geometry of the drapery shown in Figures 2a, 2b, and 2c gives $Fr = 1 + w / s$.

Solar Optical Properties of Fabric

Solar optical properties of a fabric are determined by considering what happens when beam or diffuse radiation is incident on the fabric. For radiation incident on the front surface of the fabric, the properties pertaining to transmittance are the front beam-beam transmittance $\tau_{f,bb}^m$, the front beam-diffuse transmittance $\tau_{f,bd}^m$, and the front diffuse-diffuse transmittance $\tau_{f,dd}^m$. The sum of $\tau_{f,bb}^m$ and $\tau_{f,bd}^m$ gives the front beam-total transmittance, $\tau_{f,bt}^m$. The superscript m is used to designate a fabric (i.e., material) property as opposed to the corresponding effective solar optical property of the pleated drapery. Similarly, the properties pertaining to reflectance are

the front beam-beam reflectance $\rho_{f,bb}^m$, the front beam-diffuse reflectance $\rho_{f,bd}^m$, and the front diffuse-diffuse reflectance $\rho_{f,dd}^m$. However, $\rho_{f,bb}^m$ is assumed to be 0; hence, the front beam-total reflectance, $\rho_{f,bt}^m$, is equal to $\rho_{f,bd}^m$. The corresponding properties for radiation incident on the back surface of the fabric are designated by replacing subscript f in the aforementioned nomenclature with subscript b . Refer to (Kotey et al. 2009) for more detail.

Incident Beam Radiation

Beam radiation incident on a drapery is transmitted undisturbed through fabric openings or, after multiple reflections, emerges in the forward direction as beam-diffuse transmission and in the backward direction as beam-diffuse reflection. To simplify the calculation, we consider beam-beam transmission only when beam radiation is incident on the fabric for the first time. Subsequent transmission of incident beam radiation is considered to be diffuse. This simplification is considered to be reasonable since multiple transmissions of beam radiation will entail incidence on alternating parallel or perpendicular surfaces, and one of the two (or both) incidence angles is likely to be high. At such high incidence angles, fabric beam-beam transmittance is small and the overall beam transmission will be very small.

Note that the following sections include diagrams that show only positive values of profile angle Ω_H . Recognizing the symmetry of the pleated drapery, it is apparent that the same effective properties will be obtained for positive or nega-

tive values of Ω_H . In fact, the models presented include only the absolute value of Ω_H and, because of this, apply to all values of Ω_H , ranging from -90° to $+90^\circ$.

Effective Beam-Beam Solar Optical Properties of Drapery

Consider beam radiation incident on the front (i.e., outdoor facing surface) of the drapery. The front beam-beam reflectance of the drapery, $\rho_{f,bb}$, is zero, and the front beam-beam transmittance, $\tau_{f,bb}$, can be determined by considering the three cases shown in Figure 3. The different cases are realised by considering the length of the illuminated portion of the bottom sub-enclosure, bc , relative to the width of drapery, w .

Case I ($bc \leq w$; $bc \leq ab$)

The value of Ω_H is such that surface bc is illuminated directly by incident beam radiation. Surface de is illuminated indirectly by beam radiation passing through fabric surface cd . The length of surface de is equal to the length of surface bc . Note that because of the repetitive nature of the pleats, illuminated surface bc at the bottom sub-enclosure is the same as the illuminated surface bc at the top sub-enclosure. Furthermore, incident beam radiation passing through surface bc illuminates surface ef . Since surfaces de and ef are illuminated by beam radiation that has passed through the fabric at least once, subsequent transmission of beam radiation through de and ef is considered to be diffuse. No beam radiation passes through the drapery for this case, so $\tau_{f,bb} = 0$. The condition of $\tau_{f,bb} = 0$ continues to hold as the length of bc increases until bc becomes equal to ab .

Case II ($bc \leq w$; $bc > ab$)

As Ω_H decreases and surface bc lengthens, a portion of the beam radiation passing through surface bc emerges from fictitious surface ag (see top sub-enclosure, Figure 3, Case II). The value of $\tau_{f,bb}$ is proportional to the ratio of the distance, s_1 , and the width, $2 \cdot s \cdot \cos \Omega_H$, which represents the area of incident radiation. Since the outgoing beam radiation passes through surface bc before leaving the enclosure, its strength is reduced by $\tau_{f,bb}^m$ of surface bc . Thus,

$$\tau_{f,bb} = \frac{s_1}{2 \cdot s \cdot \cos \Omega_H} \cdot \tau_{f,bb}^m(\theta_{PERP}) \quad (3)$$

It can be shown that

$$\tau_{f,bb} = \frac{(bc - eg) \cdot \sin |\Omega_H|}{2 \cdot s \cdot \cos \Omega_H} \cdot \tau_{f,bb}^m(\theta_{PERP}), \quad (4)$$

where

$$bc = s \left| \frac{\cos \Omega_H}{\sin \Omega_H} \right| \quad (5)$$

and

$$eg = w - bc. \quad (6)$$

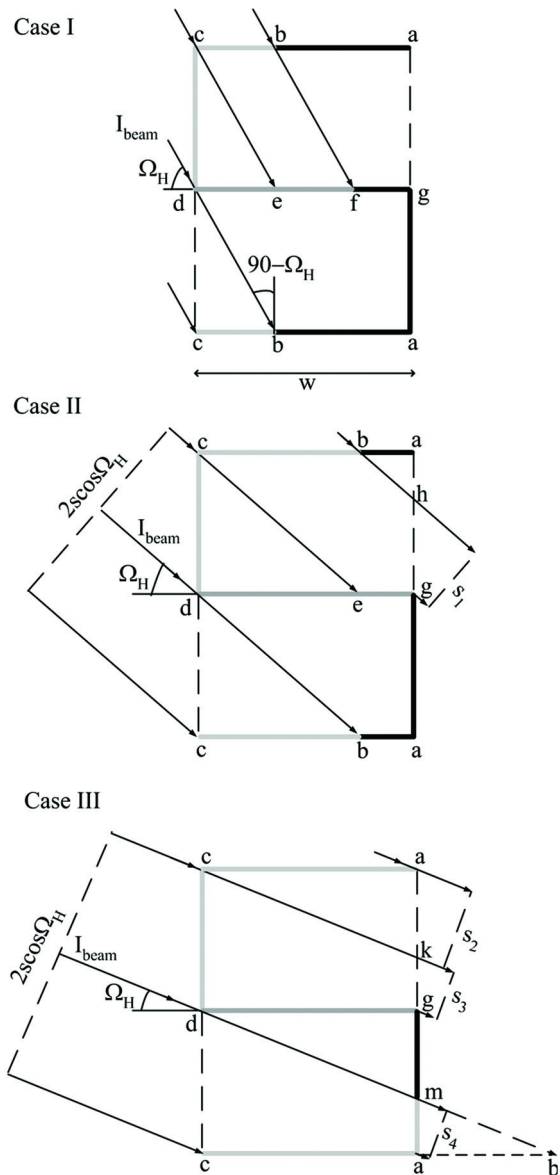


Figure 3 Calculating beam-beam effective solar transmittance of pleated drape.

The condition for one-pass beam-beam transmission continues to hold as Ω_H decreases and as bc increases until bc becomes equal to w .

Case III ($bc > w$)

When surface bc is greater than w , more beam radiation emerges from the enclosure, as shown in Figure 3, Case III. For the top sub-enclosure, beam radiation emerges from fictitious surface ag , some having passed through fabric surfaces ac and some through cd . For the bottom sub-enclosure, beam radiation is directly transmitted through fabric surface am . Note that the strength of the beam radiation on areas s_2 , s_3 , and s_4 are reduced

by $\tau_{f,bb}^m$. Fabric surfaces cd and ag are both parallel to the window with $\tau_{f,bb}^m(\theta) = \tau_{f,bb}^m(\theta_{PARL})$, whereas fabric surface ac is perpendicular to the window with $\tau_{f,bb}^m(\theta) = \tau_{f,bb}^m(\theta_{PERP})$. The value of $\tau_{f,bb}^m$ in this case is given by

$$\tau_{f,bb}^m = \frac{s_2 \cdot \tau_{f,bb}^m(\theta_{PERP}) + (s_3 + s_4) \cdot \tau_{f,bb}^m(\theta_{PARL})}{2 \cdot s \cdot \cos \Omega_H}, \quad (7)$$

which can be expressed as the following:

$$\tau_{f,bb}^m = \frac{2 \cdot (bc - w) \cdot \sin |\Omega_H| \cdot \tau_{f,bb}^m(\theta_{PARL}) + (s \cdot \cos \Omega_H - (bc - w) \cdot \sin |\Omega_H|) \cdot \tau_{f,bb}^m(\theta_{PERP})}{2 \cdot s \cdot \cos \Omega_H} \quad (8)$$

Effective Beam-Diffuse Solar Optical Properties of Drapery

Beam radiation that is intercepted by yarn and then emerges as transmitted or reflected diffuse radiation can be traced as shown in Figure 4. As seen in the previous section, the calculation can be subdivided into three cases, depending on the value of Ω_H . In all, a total of ten different surfaces can be realised between the three cases, although a minimum of seven and a maximum of nine surfaces are actually needed to analyze an individual case.

The radiant analysis can be performed with the following definitions in mind:

- J_i = radiosity of surface i
- G_i = irradiance at surface i
- $Z_{i,bb}$ = flux of beam radiation from surface i caused by beam insolation
- $Z_{i,bd}$ = flux of diffuse radiation from surface i caused by beam insolation

The following equations are applied:

$$J_{1b} = \rho_{b,dd}^m G_{1b} + \tau_{f,dd}^m G_{1f} \quad (9)$$

$$J_{2b} = Z_{2b,bd} + \rho_{b,dd}^m G_{2b} + \tau_{f,dd}^m G_{2f} \quad (10)$$

$$J_{3b} = Z_{3b,bd} + \rho_{b,dd}^m G_{3b} \quad (11)$$

$$J_{4b} = Z_{4b,bd} + \rho_{b,dd}^m G_{4b} + \tau_{f,dd}^m G_{4f} \quad (12)$$

$$J_{5b} = Z_{5b,bd} + \rho_{b,dd}^m G_{5b} + \tau_{f,dd}^m G_{5f} \quad (13)$$

$$J_{6b} = \rho_{b,dd}^m G_{6b} + \tau_{f,dd}^m G_{6f} \quad (14)$$

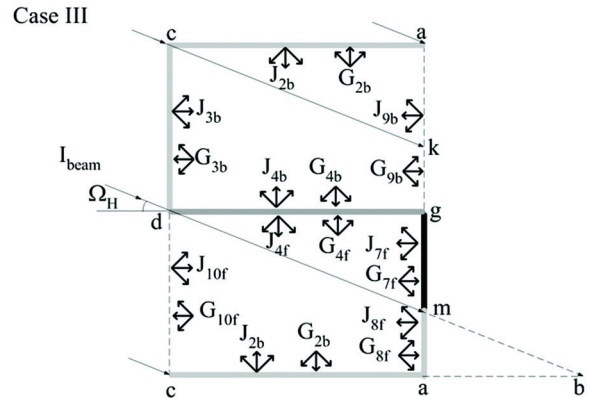
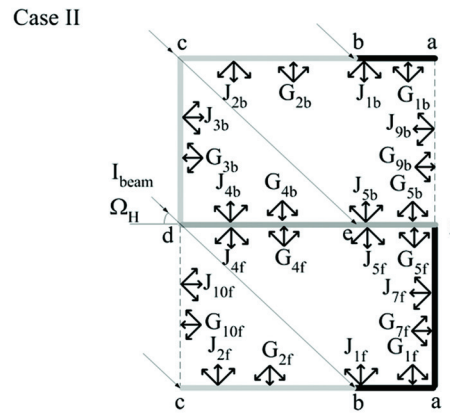
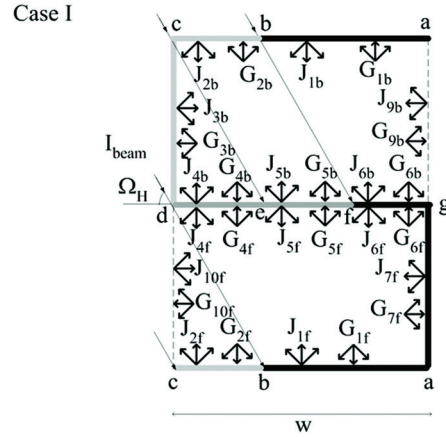


Figure 4 Calculating beam-diffuse effective solar properties of pleated drapery.

$$J_{1f} = \rho_{f,dd}^m G_{1f} + \tau_{b,dd}^m G_{1b} \quad (15)$$

$$J_{2f} = Z_{2f,bd} + \rho_{f,dd}^m G_{2f} + \tau_{b,dd}^m G_{2b} \quad (16)$$

$$J_{4f} = Z_{4f,bd} + \rho_{f,dd}^m G_{4f} + \tau_{b,dd}^m G_{4b} \quad (17)$$

$$J_{5f} = Z_{5f,bd} + \rho_{f,dd}^m G_{5f} + \tau_{b,dd}^m G_{5b} \quad (18)$$

$$J_{6f} = \rho_{f,dd}^m G_{6f} + \tau_{b,dd}^m G_{6b} \quad (19)$$

$$J_{7f} = \rho_{f,dd}^m G_{7f} \quad (20)$$

$$J_{8f} = Z_{8f,bd} + \rho_{f,dd}^m G_{8f} \quad (21)$$

Surfaces not illuminated by beam radiation do not generate a diffuse source term; hence, Z_{bd} is 0 for those surfaces. Also, the radiosities of the two fictitious surfaces ag and cd (i.e., J_{9b} and J_{10f}) are zero. It can be shown that for a given incident beam flux, I_{beam} , the beam source terms after first transmission through fabric surfaces bc and cd are as follows:

$$Z_{2b,bb} = \tau_{f,bb}^m(\theta_{PERP}) \times \frac{s}{bc} I_{beam} \quad (22)$$

$$Z_{3b,bb} = \tau_{f,bb}^m(\theta_{PARL}) \times I_{beam} \quad (23)$$

Similarly, the diffuse source terms from fabric surfaces due to I_{beam} are as follows:

$$Z_{2b,bd} = \tau_{f,bd}^m(\theta_{PERP}) \times \frac{s}{bc} I_{beam} \quad (24)$$

$$Z_{3b,bd} = \tau_{f,bd}^m(\theta_{PARL}) \times I_{beam} \quad (25)$$

$$Z_{4b,bd} = Z_{3b,bb} \times \rho_{b,bl}^m(\theta_{PERP}) \times \frac{s}{bc} \quad (26)$$

$$Z_{5b,bd} = Z_{2b,bb} \times \rho_{b,bl}^m(\theta_{PERP}) \quad (27)$$

$$Z_{2f,bd} = \rho_{f,bl}^m(\theta_{PERP}) \times \frac{s}{bc} I_{beam} \quad (28)$$

$$Z_{4f,bd} = Z_{3b,bb} \times \tau_{b,bl}^m(\theta_{PERP}) \times \frac{s}{bc} \quad (29)$$

$$Z_{5f,bd} = Z_{2b,bb} \times \tau_{b,bl}^m(\theta_{PERP}) \quad (30)$$

The diffuse irradiance on each surface of the top or bottom sub-enclosure is given by

$$G_i = \sum_j F_{ij} J_j \quad (31)$$

The view factor, F_{ij} , is the fraction of diffuse radiation leaving surface i that is intercepted by surface j . The F_{ij} can be determined by Hottel's crossed string rule (e.g., Hollands [2004]). Since all of the surfaces are flat, $F_{ii} = 0$. Likewise, F_{ij} from one surface to another surface on the same parallel or perpendicular fabric segment is 0. Note that subscripts i and j are applied to the given number of surfaces in each sub-enclosure for each particular case considered. For example, the irradiance on back of surface ac of the top sub-enclosure for Case III will be

$$G_{2b} = F_{2b2b} J_{2b} + F_{2b3b} J_{3b} + F_{2b4b} J_{4b} + F_{2b9b} J_{9b} \quad (32)$$

Equations 9 to 31 apply to all the cases shown in Figure 4. Consideration will now turn to each specific case.

Case I ($bc \leq w$; $bc \leq ab$)

As shown in Figure 4, Case I, beam radiation incident on surface bc is transmitted and reflected diffusely into the enclosure. In addition, beam radiation is transmitted diffusely through fabric surface cd . A portion of the beam radiation incident on surfaces bc and cd is transmitted directly and subsequently falls on surfaces de and ef , respectively, where it gets transmitted and reflected diffusely. Since surfaces ab , ag , and fg are shaded, no beam-to-diffuse conversion exists at these locations. Diffuse radiation in the enclosure is transmitted and reflected diffusely by all fabric surfaces. From the definitions of J , G , and Z_{bd} , a complete radiant analysis can be performed for beam-diffuse radiation using Equations 9–20 with the appropriate diffuse source terms specified in Equations 24–30. The radiosity-irradiance equation set so obtained is linear and can be solved by matrix reduction for any given I_{beam} . However, with I_{beam} set to unity, the values of $\tau_{f,bd}$ and $\rho_{f,bd}$ can be calculated as

$$\tau_{f,bd} = \frac{sG_{9b} + s\tau_{f,dd}^m G_{7f}}{2sI_{beam}} \quad (33)$$

which simplifies to

$$\tau_{f,bd} = \frac{G_{9b} + \tau_{f,dd}^m G_{7f}}{2} \quad (34)$$

and

$$\rho_{f,bd} = \frac{s\rho_{f,bl}^m(\theta_{PARL})I_{beam} + s\tau_{b,dd}^m G_{3b} + sG_{10f}}{2sI_{beam}} \quad (35)$$

which simplifies to

$$\rho_{f,bd} = \frac{\rho_{f,bl}^m(\theta_{PARL}) + \tau_{b,dd}^m G_{3b} + G_{10f}}{2} \quad (36)$$

Case II ($bc \leq w$; $bc > ab$)

As Ω_H decreases, the length of the directly illuminated surface bc increases, and the length of the indirectly illuminated surface de also increases. A portion of the beam radiation passing through surface bc escapes the enclosure through fictitious surface ag , thus leaving a smaller portion of beam radiation to fall on surface eg , as shown in Figure 4, Case II. Surface dg therefore becomes completely illuminated, while surfaces ab and ag remain shaded. A radiant analysis can be performed with the relevant equations extracted from Equations 9–20 with the corresponding diffuse source terms as specified in Equations 24–30. The set of linear equations generated can be solved by matrix reduction again with I_{beam}

set to unity. Again, the values of $\tau_{f,bd}$ and $\rho_{f,b}$ are calculated using Equations 34 and 36, respectively.

Case III ($bc > w$)

When surface bc becomes greater than w , surfaces ac and dg become completely illuminated by beam radiation. A portion of fabric surface ag (i.e., surface 8f) is also illuminated directly by beam radiation. The only surface that is shaded is mg . A significant portion of the beam radiation passing through fabric surfaces ac and cd and fictitious surface cd escapes the enclosure as beam radiation. With the relevant relations extracted from Equations 9–21 and the appropriate diffuse source terms as specified in Equations 24–30, the set of linear equations so generated can be solved. Again, with I_{beam} set to unity, the value of $\tau_{f,bd}$ is calculated as

$$\tau_{f,bd} = \frac{sG_{9b} + \tau_{f,dd}^m \times (gm \times G_{7f} + am \times G_{8f}) + am \times \tau_{f,bd}^m(\theta_{PARL})}{2} \quad (37)$$

where

$$gm = w \left| \frac{\sin \Omega_H}{\cos \Omega_H} \right| \quad (38)$$

and

$$am = s - gm. \quad (39)$$

Likewise, the value of $\rho_{f,bd}$ can be calculated from Equation 36.

Effective Diffuse-Diffuse Solar Optical Properties of Drapery

Consider diffuse radiation, I_{diff} , incident on the front of the drapery layer (see Figure 5). Diffuse radiation within the enclosure remains diffuse as it interacts with the surfaces before finally emerging in the forward (transmission) and backward (reflection) direction. The values of $\tau_{f,dd}$ and $\rho_{f,dd}$ can be determined by considering the representative geometry (w and s). In this particular situation, the calculations are independent of θ and Ω_H . The following equations are applied:

$$J_{2b} = \rho_{b,dd}^m G_{2b} + \tau_{f,dd}^m G_{2f} \quad (40)$$

$$J_{3b} = \tau_{f,dd}^m I_{diff} + \rho_{b,dd}^m G_{3b} \quad (41)$$

$$J_{4b} = \rho_{b,dd}^m G_{4b} + \tau_{f,dd}^m G_{4f} \quad (42)$$

$$J_{2f} = \rho_{f,dd}^m G_{2f} + \tau_{b,dd}^m G_{2b} \quad (43)$$

$$J_{4f} = \rho_{f,dd}^m G_{4f} + \tau_{b,dd}^m G_{4b} \quad (44)$$

$$J_{8f} = \rho_{f,dd}^m G_{8f} \quad (45)$$

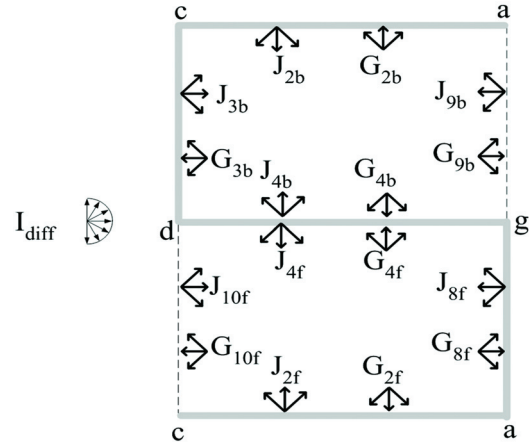


Figure 5 Calculating diffuse-diffuse effective solar properties of pleated drapery.

The radiosity of fictitious surface cd is $J_{10f} = I_{diff}$, while the radiosity of fictitious surface ag is $J_{9b} = 0$. The irradiance on each surface of either sub-enclosure can be calculated using Equation 31, with the subscripts i and j applied to the given number of surfaces in that sub-enclosure. Once again, Equations 40–45 are linear and can be solved by matrix reduction with I_{diff} set to unity. The values of $\tau_{f,dd}$ and $\rho_{f,dd}$ are as follows:

$$\tau_{dd} = \frac{G_{9b} + \tau_{f,dd}^m G_{8f}}{2} \quad (46)$$

$$\rho_{f,dd} = \frac{\rho_{f,dd}^m + \tau_{b,dd}^m G_{3b} + G_{10f}}{2} \quad (47)$$

Back Effective Solar Optical Properties of Drapery

In the preceding sections, models were described for the calculation of front effective solar optical properties of a pleated drapery. The corresponding back-surface properties can be calculated using the same models by interchanging the front and back fabric properties.

RESULTS AND DISCUSSION

The Present Model

Nominal property data for the nine fabric designations presented in Keyes's chart (Keyes 1967; ASHRAE 2005) were obtained from Keyes (1967). These data are listed in Table 1. It is assumed that front and back properties are equal, so the subscripts f and b have been dropped for simplicity. At normal incidence, $\tau_{bb}^m(\theta = 0)$ is equivalent to the openness factor, A_o (Keyes 1967). The value of $\tau_{bd}^m(\theta = 0)$ corresponds to radiation redirected by the yarn in the forward direction. The sum of the two, the total transmittance of the fabric, $\tau_{bt}^m(\theta = 0)$, corresponds to the vertical axis in Keyes's chart. As expected, the closed weave fabrics have negligible τ_{bb}^m while the open and

Table 1. Nominal Solar Properties of Drapery Fabrics

Fabric Designation	Fabric Description	Beam-Beam Transmittance	Beam-Diffuse Transmittance	Beam-Total Transmittance	Beam-Total Reflectance
I_D	Open weave, dark-coloured	0.35	0.04	0.39	0.07
II_D	Semi-open weave, dark-coloured	0.15	0.03	0.18	0.10
III_D	Closed weave, dark-coloured	0.01	0.04	0.05	0.14
I_M	Open weave, medium-coloured	0.35	0.14	0.49	0.25
II_M	Semi-open weave, medium-coloured	0.15	0.14	0.29	0.32
III_M	Close weave, medium-coloured	0.01	0.10	0.11	0.38
I_L	Open weave, light-coloured	0.35	0.23	0.58	0.36
II_L	Semi-open weave, light-coloured	0.15	0.26	0.41	0.48
III_L	Close weave, light-coloured	0.01	0.16	0.17	0.63

semi-open weave fabrics allow some beam-beam transmission. Furthermore, in each openness category, the light-coloured fabrics have the highest ρ_{bt}^m , followed by the medium-coloured fabrics, while the dark-coloured fabrics have the lowest ρ_{bt}^m .

The effective solar properties of the drapery were calculated for both incident beam and incident diffuse radiation. The results are shown in Figures 6a and 6b, grouped into open weave (I), semi-open weave (II), and closed weave (III) categories. Subgroupings show transmittance and reflectance for light-coloured (L), medium-coloured (M), and dark-coloured (D) draperies. Figure 6a shows the variation of the τ_{dd} and ρ_{dd} with Fr for all nine fabric designations. Note that for $w = 0$ ($Fr = 1$), the drape is flat and the effective properties of the drape correspond to the properties of the fabric.

It can be seen that τ_{dd} for draperies with open and semi-open fabrics decreases with increasing Fr , while the value of τ_{dd} for draperies with closed-weave fabrics remains nearly constant. This trend is found in all three colour designations. It is to be expected that pleating will consistently decrease solar transmission because there is more opportunity for radiation to be absorbed in the fabric because of the interreflection that arises if the fabric can view itself.

The calculated ρ_{dd} data reveal another interesting phenomenon. For open weave, light-coloured drapery (I_L), pleating causes ρ_{dd} to increase at $Fr < 3$. Again, this is due to self-viewing. Some of the radiation that passes through the front surface of the drape (fabric surface cd) will encounter one of the perpendicular surfaces (dg or ac), where a portion will transmit to the adjacent cavity and a portion of this radiation will exit through the opening (fictitious surface cd), either directly or by intermediate reflection. This effect is most prevalent in fabrics with higher values of A_o and yarn reflectance. Open weave, medium-coloured drapery (I_M) shows a slight decrease in ρ_{dd} , while for open weave, dark-coloured drapery (I_D), ρ_{dd} remains almost constant at a small value. For semi-open and closed weave draperies, ρ_{dd} decreases with increasing Fr irrespective of the colour of the drapery.

Now consider the effect of Ω_H on the solar properties of draperies. To investigate this effect, Ω_V was fixed at 0 and $Fr = 2$ (100% fullness) was chosen. The results are shown in Figure 6b. Clearly, τ_{bb} for open and semi-open weave draperies always decreases with increasing Ω_H . At $\Omega_H = 63.4^\circ$, the cutoff angle that marks the transition from Case II to Case III for the 100% fullness drapery, τ_{bb} is completely eliminated. An increase in Ω_H beyond this cutoff angle results in only beam-diffuse transmission through the drapery. It should be noted that a small amount of beam-beam transmission through a drapery would be predicted with Ω_H greater than the cutoff angle if multiple beam-beam transmissions through the fabric were considered. For closed weave drapes (type III), $\tau_{bb}^m(\theta = 0) \approx 0$, and τ_{bb} is very close to 0 for all values of Ω_H . Generally, τ_{bd} for open-weave drapery (type I) shows a weak increase to a local maximum at the cutoff angle and then decreases as Ω_H increases further. On the other hand, τ_{bd} for semi-open and closed weave drapery (types II and III) decreases gradually with an increase in Ω_H over the full range of Ω_H .

Turning to the variation of ρ_{bd} with Ω_H , note that draperies in all nine fabric designations exhibit an increase in ρ_{bd} as Ω_H increases. This increase in ρ_{bd} happens for two reasons. First, the solar reflectance of the exposed front surface of the drapery, surface $3f$, increases as Ω_H increases. Second, as Ω_H increases, the illuminated portion of the lower cavity, surface $2f$, moves closer to the front face of the pleated drapery and more of the solar radiation reflected from this section of fabric will exit through the front opening as reflection from the pleated drapery.

Comparison with the Farber et al. (1963) Model

Farber et al. (1963) produced curves of effective reflectance versus Fr for incident diffuse radiation. Figure 7a shows curves reproduced from Farber et al. for values of ρ_{dd} ranging from 0.1 to 0.5. Since no information was given to the contrary, it is assumed that these fabrics were opaque. The curves clearly show a decrease in ρ_{dd} as Fr increases. This is the

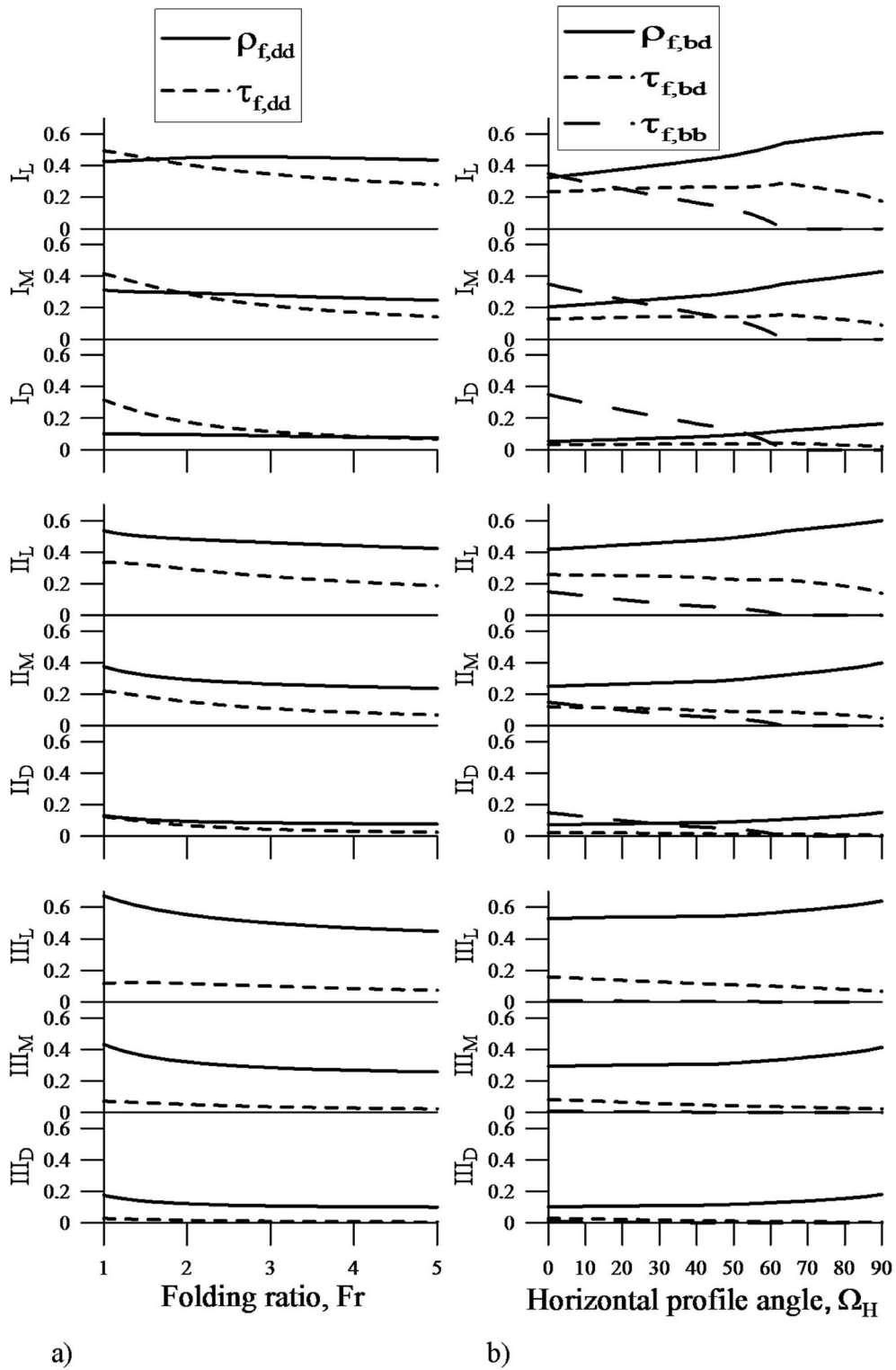


Figure 6 Effective solar drapes properties: a) diffuse and b) beam, 100% fullness.

expected trend for fabrics with low solar transmittance. The curves also show that the higher the value of ρ_{dd}^m , the stronger the influence of Fr . Results generated with the present model, Figure 7b, compare favourably with Figure 7a. Both models predict $\rho_{dd} = \rho_{dd}^m$ at $Fr = 1$, which corresponds to a pleatless (flat) drape. At high values of Fr , the present model predicts slightly lower values of ρ_{dd} , especially for fabrics with high values of ρ_{dd}^m . In general, and particularly for the most practical cases at $Fr \leq 2$, the agreement is very good.

Now compare the two models for incident beam radiation. Farber et al. (1963) generated curves of effective transmittance and absorptance for a 100% fullness drapery versus θ . They considered three different shades of drapery: dark-coloured (tan), medium-coloured (grey), and light-coloured (white). The solar optical properties of the three shades of fabric at normal incidence are summarised in Table 2. The transmittance and reflectance values shown in Table 2 should be interpreted as $\tau_{bt}^m(\theta = 0)$ and $\rho_{bb}^m(\theta = 0) = \rho_{bd}^m(\theta = 0)$. The Farber et al. model uses the assumption that the fabrics transmit and reflect diffusely: $\tau_{bb}^m = 0$, $\tau_{bt}^m = \tau_{bd}^m$, and $\rho_{bb}^m = 0$. In contrast, the current model allows for the possibility of direct beam transmission through openings in the fabric, but a value for $\tau_{bb}^m(\theta = 0) = A_o$ must also be supplied. Noting that the light-coloured, medium-coloured, and dark-coloured fabrics in question have approximately the same solar reflectance, it must be concluded that they have different amounts of openness. The values of A_o used in the current model are also listed in Table 2. These A_o values were read from the Keyes (1967) chart using the given values of $\tau_{bt}^m(\theta = 0)$ and $\rho_{bt}^m(\theta = 0)$.

The Farber et al. (1963) model required input data describing the variation of fabric reflectance and transmittance with respect to θ (see Figure 8a, reproduced from Farber et al. [1963]). To compare the Farber et al. drapery model with the present model, the corresponding reflectance curves for the three fabrics were generated using the fabric model documented in Kotey et al. (2009)—the same fabric model used throughout the current study. The results are shown in Figure 8b. With the exception of the grey fabric, there is good agreement between the two sets of fabric reflectance curves. No information was given as to how Farber et al. obtained the curves shown in Figure 8a.

Figures 9a, 10a, and 11a show calculated values of effective absorptance and transmittance versus θ for tan, grey, and white draperies, reproduced from Farber et al. (1963). Results

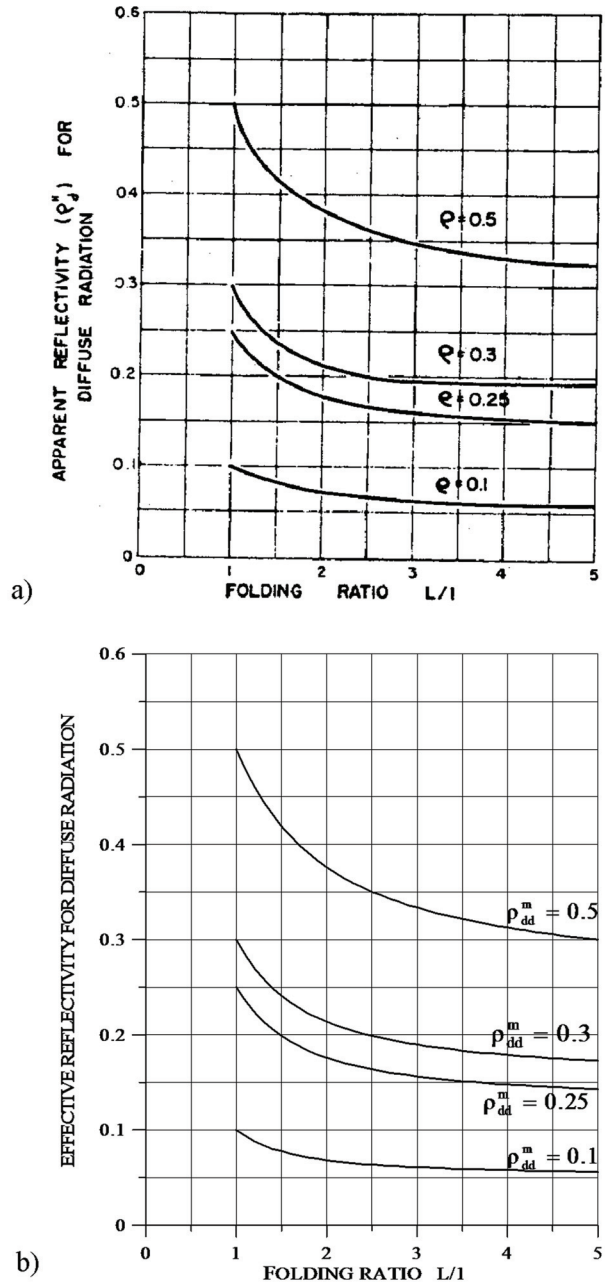
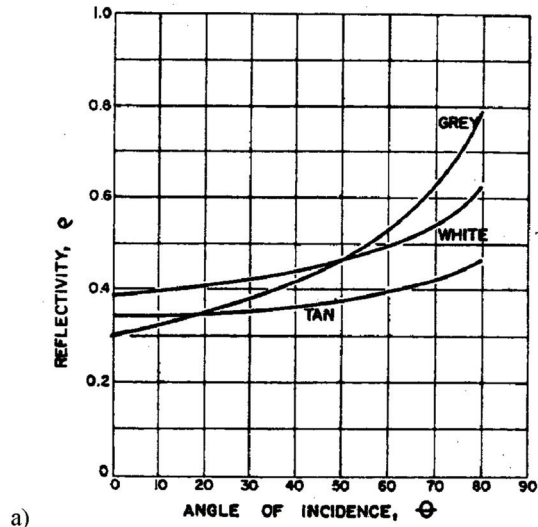


Figure 7 Effective diffuse-diffuse reflectance of pleated drape: a) Farber et al. (1963) model; b) the present model.

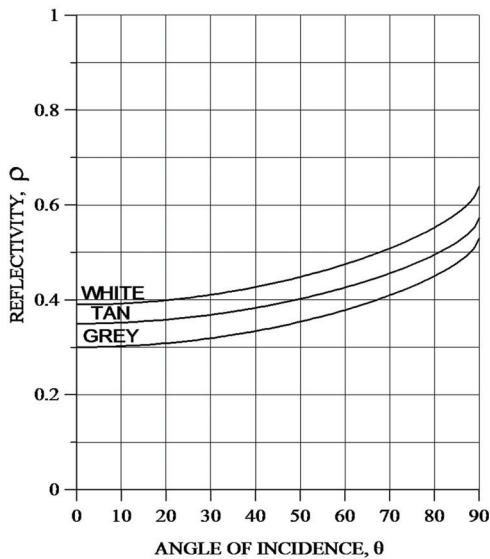
Table 2. Solar Optical Properties for Dark-Coloured, Medium-Coloured, and Light-Coloured Fabrics, Normal Incidence (Farber et al. 1963)

Fabric Description	Transmittance	Reflectance	Absorptance	Openness*
Dark-coloured (tan)	0.14	0.35	0.51	0.03
Medium-coloured (grey)	0.23	0.30	0.47	0.12
Light-coloured (white)	0.35	0.39	0.26	0.16

* Note: Openness estimated using Keyes's (1967) chart (ASHRAE 2005).



a)

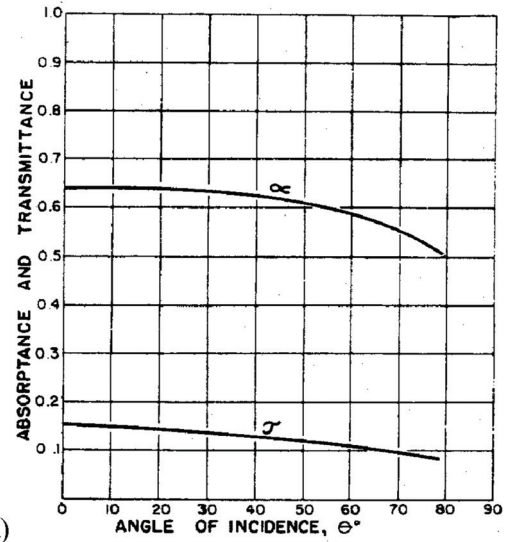


b)

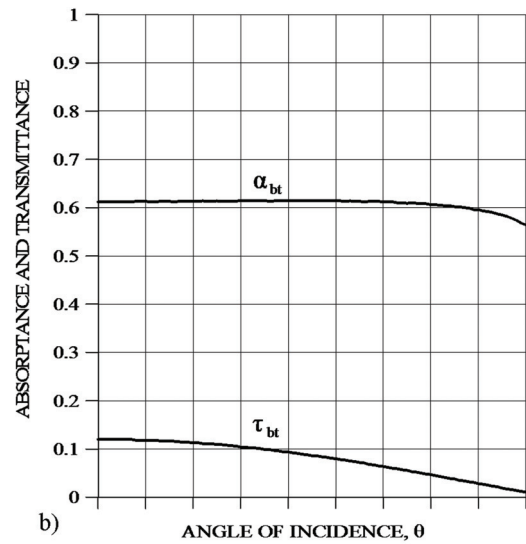
Figure 8 Reflectivity of fabrics versus angle of incidence: a) Farber et al. (1963) model; b) Kotey et al. (2009) model.

from the present model are shown for comparison in Figures 9b, 10b, and 11b. In producing Figures 9, 10, and 11, the horizontal projection angle was fixed at $\Omega_H = 0$, so $\theta = \Omega_V$.

In general, the agreement is good, given the limitations of the Farber et al. (1963) model. Results for the dark-coloured drapery agree very well. The results for the medium-coloured drapery agree well at $\theta = 0$, but a significant discrepancy in absorptivity is seen at off-normal incidence. This is clearly due to the unusual off-normal property curve shown in Figure 8a for the grey fabric and possibly the inability of the Farber et al. model to account for openness ($A_o = 0.12$). Figure 11 shows noticeable discrepancies between the two models for light-coloured drapes. Various reasons can be offered to explain



a)

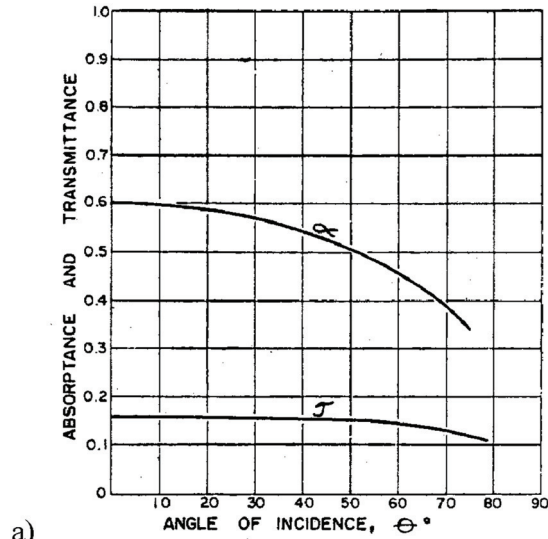


b)

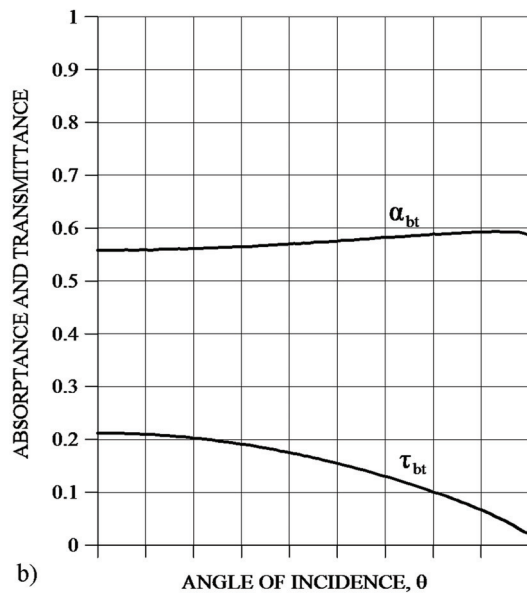
Figure 9 Effective transmittance and absorptance of dark-coloured (tan) drape versus angle of incidence ($\theta = \Omega_V$): a) Farber et al. (1963) model; b) the present model.

these differences, including the openness of the white fabric ($A_o = 0.16$), but the comparison is probably not legitimate in this case. Examining Figure 11a, the Farber et al. model predicts a transmittance of 42% for a pleated drape made from fabric with 35% transmittance. These data indicate a problem because pleating will always reduce solar transmittance, as shown in Figure 6a. It is not clear whether the Farber et al. model was applied incorrectly for the white drape or if perhaps the labels (α and τ) should be interchanged in Figure 11a.

To further explore the effect of pleat geometry, the current model was used to generate results for the three fabrics examined by Farber et al. (1963). Solar properties were calculated



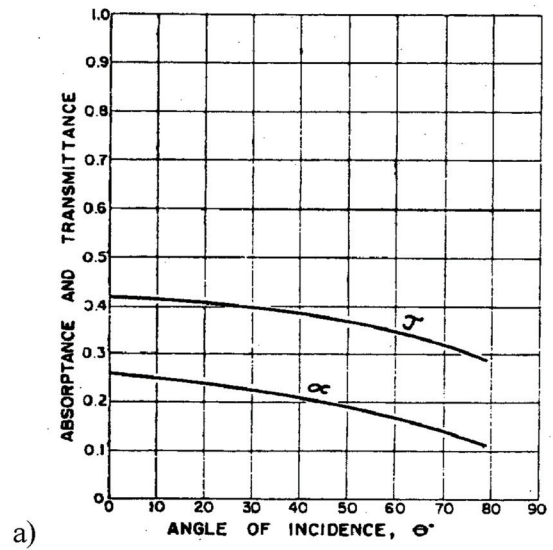
a)



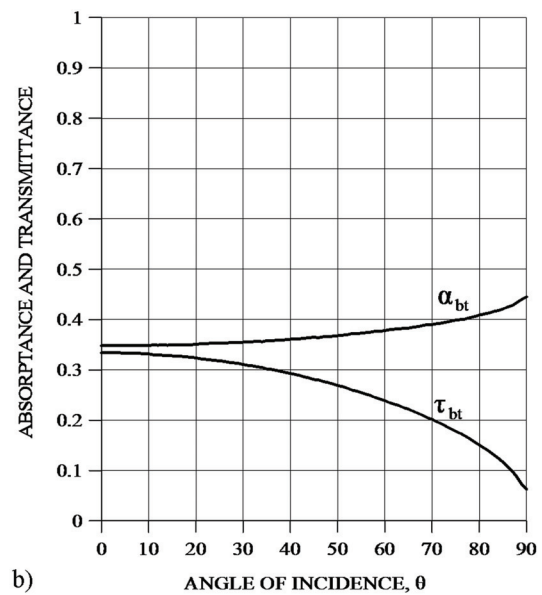
b)

Figure 10 Effective transmittance and absorptance of medium-coloured (tan) drape versus angle of incidence ($\theta = \Omega_V$): a) Farber et al. (1963) model; b) the present model.

for pleated drapes with 100% fullness, and properties for both drape (solid lines) and fabric (dashed lines) are shown with respect to the horizontal projection angle ($\Omega_V = 0$ and $\Omega_H = \theta$) in Figure 12. Compared to a flat fabric, pleating causes the incident radiation to interact with the fabric surfaces via multiple reflections and transmissions. This interaction generally gives rise to higher absorptance, lower reflectance, and lower transmittance (as asserted above regarding Figure 11a) of a pleated drape compared to the flat fabric. Figure 12 shows these relations to be true for the three fabrics examined over virtually the full range of incidence angle.



a)



b)

Figure 11 Effective transmittance and absorptance of light-coloured (tan) drape versus angle of incidence ($\theta = \Omega_V$): a) Farber et al. (1963) model; b) the present model.

On a more general note, Moore and Pennington (1967) acknowledged difficulty in measuring the effective solar properties of draperies. Given the solar properties of a fabric at normal incidence, they proposed constants that could be used to scale down the solar properties of the fabric in order to obtain the effective solar optical properties of the drapery. Their scaling constants were based on experiments performed with several fabrics. The present results, however, show that the solar properties of a pleated drape do not necessarily decrease by a constant factor with respect to Fr and/or θ . In fact, depending on the combination of fabric properties Fr and

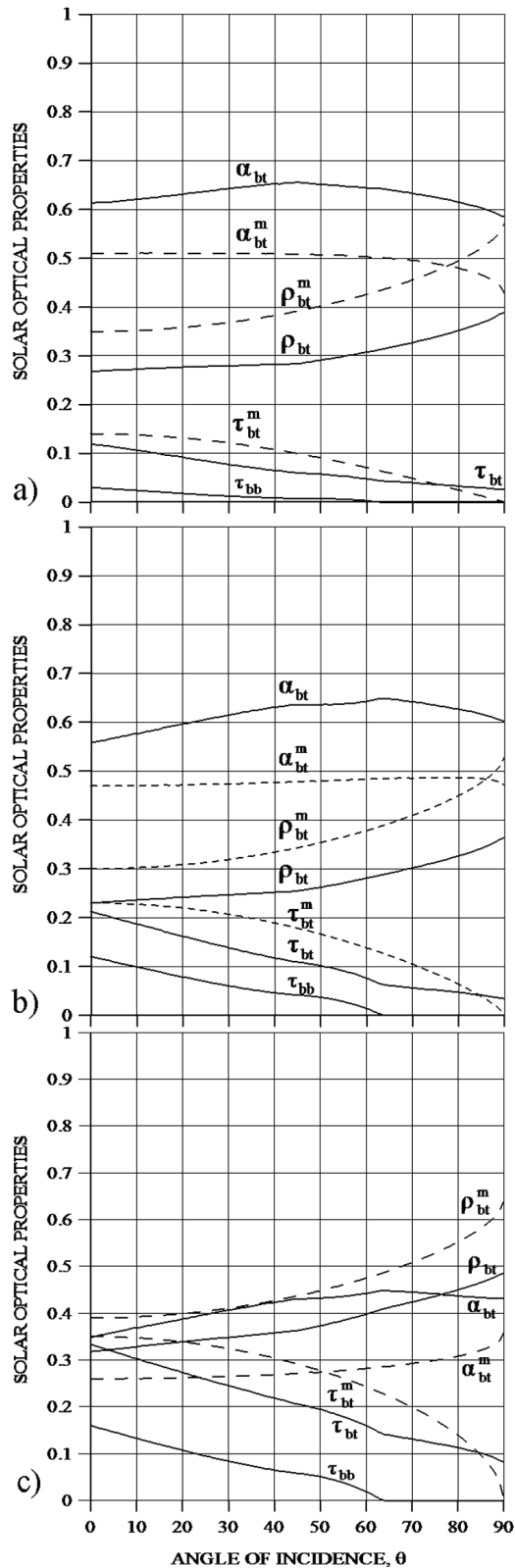


Figure 12 Solar properties of pleated drapes and fabrics versus incidence angle ($\Omega_V = 0$ and $\Omega_H = \theta$) for yarn colours a) tan, b) grey, and c) white.

θ , the effective solar properties of the drape could be greater than the corresponding properties of the fabric.

CONCLUSIONS

A detailed model was developed to calculate the effective solar properties of pleated drapes. The model approximates a drape as a series of uniform rectangular pleats. The pleated drape model then uses angle-dependent properties of the flat fabric (Kotey et al. 2009) in conjunction with drapery geometry and solar angles to calculate the effective solar properties for both incident beam and diffuse radiation. The model is general enough to handle open weave fabrics, allowing for beam-beam transmission. The model compares favourably with models documented in the literature. The results obtained from the present model also show that the solar optical properties of a drapery do not always decrease by a factor with respect to folding ratio and/or incidence angle, as was suggested by previous researchers. A model for determining properties of pleated drapes is particularly useful in the multi-layer analysis of windows. In turn, this capability applied to computer-based building energy simulation offers the opportunity to predict peak cooling load reduction and energy savings associated with the use of drapes.

ACKNOWLEDGMENTS

Financial support from the Natural Science and Engineering Research Council and the American Society of Heating, Refrigerating and Air-Conditioning Engineers, Inc., is gratefully acknowledged.

REFERENCES

- ASHRAE. 2005. *2005 ASHRAE Handbook—Fundamentals*. Atlanta: American Society of Heating, Refrigerating and Air-Conditioning Engineers, Inc.
- Farber, E.A., W.A. Smith, C.W. Pennington, and J.C. Reed. 1963. Theoretical analysis of solar heat gain through insulating glass with inside shading. *ASHRAE Journal*, pp. 79.
- Hollands, K.G.T. 2004. *Thermal Radiation Fundamentals*. New York: Begell House, Inc.
- Keyes, M.W. 1967. Analysis and rating of drapery materials used for indoor shading. *ASHRAE Transactions* 73(1):8.4.1.
- Kotey, N.A., J.L. Wright, and M.R. Collins. 2007. A simplified method for calculating the effective solar optical properties of a drapery. *Proceedings of the 32nd Conference of the Solar Energy Society of Canada Inc. (SESCI) and 2nd Conference of the Solar Building Research Network (SBRN), Calgary, Alberta, Canada, June 9–13, 2007*.
- Kotey, N.A., J.L. Wright, and M.R. Collins. 2009. Determining off-normal solar optical properties of drapery fabrics. *ASHRAE Transactions*. In review.

- Moore, G.L., and C.W. Pennington. 1967. Measurement and application of solar properties of drapery shading materials. *ASHRAE Transactions* 73(1):8.3.1.
- Ozisik, N., and L.F. Schutrum. 1960. Solar heat gain factors for windows with drapes. *ASHRAE Transactions* 66:228.
- Pennington, C.W., W.A. Smith, E.A. Farber, and J.C. Reed. 1964. Experimental analysis of solar heat gain through insulating glass with indoor shading. *ASHRAE Journal* 2:27.
- Sparrow, E.M., and V.K. Johnson. 1962. Thermal radiation absorption in rectangular grooves. ASME paper 62-WA-52.
- Wright, J.L., and N.A. Kotey. 2006. Solar absorption by each element in a glazing/shading layer array. *ASHRAE Transactions* 112(2):3–12.
- Wright, J.L. 2008. Calculating centre-glass performance indices of glazing systems with shading devices. *ASHRAE Transactions* 114(2).
- Yellot, J.I. 1965. Drapery fabrics and their effectiveness in solar heat control. *ASHRAE Transactions* 71(1):260–72.